PAPER • OPEN ACCESS

Enhanced lifetimes of spin chains coupled to chiral edge states

New Journal of Physics
The open access journal at the forefront of physics

Deutsche Physikalische Gesellschaft DPG
IOP Institute of Physics

Published in partnership with: Deutsche Physikalische Gesellschaft and the Institute of Physics

OPEN ACCESS

RECEIVED
15 November 2018

REVISED
7 March 2019

ACCEPTED FOR PUBLICATION
20 March 2019

PUBLISHED
8 April 2019

PAPER

Enhanced lifetimes of spin chains coupled to chiral edge states

F Delgado[1] and J Fernández-Rossier[2,3]

[1] Instituto de estudios avanzados IUDEA, Departamento de Física, Universidad de La Laguna, C/Astrofísico Francisco Sánchez, s/n. E-38203, La Laguna, Spain
[2] QuantaLab, International Iberian Nanotechnology Laboratory (INL), Av. Mestre José Veiga, 4715-310 Braga, Portugal
[3] Departamento de Física Aplicada, Universidad de Alicante, Spain

E-mail: fernando.delgado@ull.edu.es

Keywords: spin Hall, decoherence, relaxation, adatoms, Kondo

Abstract

We consider spin relaxation of finite-size spin chains exchanged coupled with a one-dimensional (1D) electron gas at the edge of a quantum spin Hall (QSH) insulator. Spin lifetimes can be enhanced due to two independent mechanisms. First, the suppression of spin-flip forward scattering inherent in the spin momentum locking of the QSH edges. Second, the reduction of spin-flip backward scattering due to destructive interference of the quasiparticle exchange, modulated by $k_F d$, where d is the inter-spin distance and k_F is the Fermi wavenumber of the electron gas. We show that the spin lifetime of the $S = 1/2$ ground state of odd-numbered chains of antiferromagnetically coupled $S = 1/2$ spins can be increased more than 4 orders of magnitude by properly tuning the product $k_F d$ and the spin size N, in strong contrast with the 1D case. Possible physical realizations together with some potential issues are also discussed.

1. Introduction

The study of both individual spins [1–3] and their engineered structures [2, 4–8] deposited on surfaces entails the interaction of these surface spins with the underlying electron gas of the substrate. These systems can be built and probed using an scanning tunneling microscope (STM). Moreover, recent experiments [8–11] show that single spin resonance experiments can be carried out with STM. However, in order to achieve coherent manipulation of the surface spins it would be necessary to increase the spin lifetime T_1 and spin coherence T_2 beyond the inverse of the Rabi coupling, a condition that is not met in these systems.

The spin lifetime of individual magnetic atoms is controlled by the electronic properties of the substrate, the surface spin system, and their exchange interaction, encoded in ρJ, where J is the Kondo exchange and ρ is the substrate density of states [12–14]. The enhancement of spin-lifetimes by reduction of either ρ or J has been has been explored in several systems, including heavy metal substrates with strong spin–orbit [15], superconducting [16] or semiconducting [3] surfaces and thin decoupling layers, such as Al_2O_3 on NiAl [1], Cu_2N on Cu(100) [17] or MgO/Ag(100) [18]. Relaxation times for 3d atoms on metals range from the ps time scale for magnetic atoms directly on a conducting substrate [19] up to tens of ms [20] in the presence of a decoupling layer. In addition, the role of the symmetry of the adsorption site have been highlighted [21–24]. This has permitted reaching the single atom limit *bit* by depositing Ho atoms on a MgO/Ag(100) surface [10, 23] with relaxation times exceeding hours observed.

Spin arrays offer additional routes to control their spin lifetimes, compared to individual spins on surfaces. For instance, transitions between the two ground states of magnetically ordered short spin chains, either ferro or antiferromagnetically (AFM) coupled, are severely slowed down [6, 7]. A drawback of this approach is that it essentially relies on building larger objects for which decoherence is much faster. Therefore, larger T_1 comes at the expense of a much shorter T_2. A second route for engineering the spin lifetimes of spin arrays is to take advantage of the destructive interference in the scattering between substrate quasiparticles and an ordered array of spins [25].

More specifically, in a previous work [25] we found that spin relaxation of linear spin arrays interacting with a one-dimensional (1D) electron gas has an oscillatory dependence on $k_F d$. In this case, the spin relaxation has two contributions attending to the momentum transfer of the quasiparticle, forward and backward scattering, each of which has both spin-flip and spin-conserving processes. Here we propose to use the peculiar spin-locking of the quasiparticles at the edges of a quantum spin Hall (QSH) [26] to enhance the T_1 in engineered spin chains. For the the edge states of the QSH insulator, spin-conserving quasiparticle scattering is only possible in the forward channel, and spin-flip scattering requires back-scattering, see figure 1. Therefore, this already reduces half of the scattering channels. The scope of this work is to show how spin-flip back-scattering can be further reduced, or even fully suppressed, by engineering $k_F d$, either by atomic positioning (changing d) or by gating (changing k_F).

The QSH phase was first observed in heterostructures of HgTe/CdTe [27], following a prediction of Bernevig *et al* [28]. Strong evidence of QSH phase has been found on heterostructures of InAs/GaInSb [29]. However, the QSH edges are buried inside a heterostructure, making it almost impossible to carry out STM manipulation/deposition of magnetic atoms in these systems. Edge states have been observed with STM in atomically thin islands of Bi (111) [30, 31], although there is still some controversy about the evidences of spin-locked edge states [32, 33]. Recently, the observation of the QSH effect has been reported on a monolayer crystal of WTe_2 [34, 35] showing a robust topological phase up to 100 K [36].

The interplay between local moments and itinerant QSH edge quasiparticles has been extensively studied theoretically [37–41]. Most of the previous works have focused on the impact of local spins, either magnetic impurities or nuclei, on the quasiparticle spin relaxation, which has a direct impact on the lack of conductance quantization: in the absence of spin-flip scattering, the conductance of QSH channels should be e^2/h [26]. Experiments [27, 29, 34, 36] very often find smaller conductance values, which motivates the quest of spin-flip back-scattering mechanisms [29, 34]. There are in addition several proposals for the manipulation of nanomagnets and local magnetic impurities with the spin-transfer torque exerted by the fully spin-polarized current of QSH edges [42–44]. Here we focus on the relaxation and decoherence of the spin states of magnetic chains, putting special emphasis on the role of scattering interference.

The rest of this manuscript is organized as follows. In section 2 we describe the model Hamiltonian that describe the spin chain, the electron gas hosted at an edge of a QSHI, and their Kondo interaction. In section 3 we revisit the expressions for the relaxation T_1^{-1} and decoherence T_2^{-1} rates. . The dissipative dynamics of a $S = 1/2$ degree of freedom encoded in the ground state doublet of odd-numbered chain of AFM coupled $S = 1/2$ spins is discussed in section 4. Finally, a thorough discussion of the results and the main conclusions are presented in section 5.

2. System Hamiltonian

Let us consider a linear chain of N equidistant magnetic adatoms, with inter-atom distance d, deposited on equivalent atomic adsorption sites described by the spin Hamiltonian $\mathcal{H}_{\rm chain} = J_{\rm H}\sum_l \vec{S}(l)\cdot\vec{S}(l+1) + \mathcal{H}_{\rm Zeem}$ where $\vec{S}(l)$ is the spin of the l-magnetic adatom. The first term accounts for the Heisenberg exchange coupling and the last one for the Zeeman interaction with an external magnetic field. We will denote by $|M\rangle$ and $E_{\rm M}$ the eigenvectors and eigenvalues of $\mathcal{H}_{\rm chain}$. We will focus our discussion on the simplest $S = 1/2$ case, and thus the magnetocrystalline anisotropy will not be discussed unless otherwise stated.

In the proximity of a conductor, the local spins suffer a Kondo exchange interaction with the conduction electrons [45]: $\mathcal{V}_K = \sum_i^N \mathcal{J}_l \vec{S}(l)\cdot\vec{s}(\vec{\eta})$, where $\vec{s}(\vec{\eta})$ is the surface spin density evaluated at the position $\vec{\eta}$ of the l-magnetic atom [13, 25]. Here we are interested in the case where the *conductor* is substituted by a *chiral 1D edge state*.

Spin relaxation of local spins due to Kondo exchange with itinerant quasiparticles is governed by states in the neighborhood of the Fermi energy. We model these states as left and right moving quasiparticles with linear dispersion $\epsilon_k - \epsilon_F = \pm\hbar v_F k$, where v_F is the Fermi velocity and k the momentum measured with respect to $\mp k_F$, with k_F the Fermi wavenumber. Taking into account the spin-momentum locking, we define the field operators

$$\Psi_\uparrow^\dagger(x) \approx \frac{e^{ik_F x}}{\sqrt{L}}\sum_k e^{ikx} R_k^\dagger$$
$$\Psi_\downarrow^\dagger(x) \approx \frac{e^{-ik_F x}}{\sqrt{L}}\sum_k e^{-ikx} L_k^\dagger, \quad (1)$$

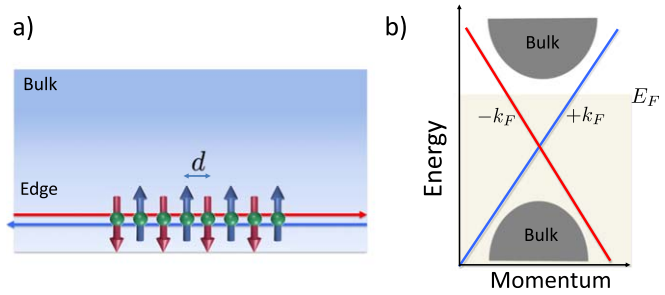

Figure 1. Scheme of the physical system. (a) A linear antiferromagnetic Heisenberg chain of $S = 1/2$ spins is deposited on the edge of an spin Hall bar (SHB). For a given edge, electrons with spin up move in opposite direction to those with spins down. (b) Schematic representation of the energy bands of the SHB. The two chiral edge states, for which spin and momentum are locked, present a linear dispersion close to the Fermi level.

where L is the length of the edge and $L_k^\dagger \equiv c^\dagger_{-(k_F+k),\downarrow}$ and $R_k^\dagger \equiv c^\dagger_{+(k_F+k),\uparrow}$ are the left (right) moving fermion operators, with $c^\dagger_{k\sigma}$ the creation operator of a fermion in the edge channel with spin σ and momentum k[4]. We assume that the quasiparticle spins have a momentum independent quantization axis, that we denote as the z axis. This assumption is met in the Kane–Mele model [26], but in real materials it could fail. We can now write the non-interacting Hamiltonian of the QSH edge quasiparticles close to the Fermi energy reads as:

$$\mathcal{H}_{\rm edge} = \hbar v_{\rm F} \sum_k [(k_{\rm F} + k) R_k^\dagger R_k - (k_{\rm F} + k) L_k^\dagger L_k], \tag{2}$$

where $v_{\rm F}$ is the Fermi velocity, which is the same for left and right goers on account of time reversal symmetry. Here the sum over k is restricted to a small window around $k = 0$ where the linear dispersion relation holds.

A spin chain coupled to one edge state of a SHB can be described by the following Hamiltonian $\mathcal{H} = \mathcal{H}_{\rm chain} + \mathcal{H}_{\rm edge} + \mathcal{V}_K$, where the resulting Kondo coupling has two different contributions, $\mathcal{V}_K^\parallel + \mathcal{V}_K^\perp$, where

$$\mathcal{V}_K^\parallel = \sum_l \frac{J_l}{2L} \hat{S}^z(l) \sum_{kk'} {\rm e}^{{\rm i}(k-k')dl} (R_k^\dagger R_{k'} - L_{-k}^\dagger L_{-k'}) \tag{3}$$

and

$$\mathcal{V}_K^\perp = \sum_{l,k,k'} \frac{J_l}{2L} (\hat{S}^+(l) {\rm e}^{{\rm i}(2k_{\rm F}+k+k')dl} L_k^\dagger R_{k'} + {\rm h.c.}), \tag{4}$$

where we have introduced the spin-ladder operators $\hat{S}^\pm = 1/2(\hat{S}^x \pm {\rm i}\hat{S}^y)$. The first term $\mathcal{V}_K^\parallel$ corresponds to the spin-conserving Ising-like term. The second term will be responsible of the spin-flips. Importantly $\mathcal{V}_K^\parallel$ contains only forward scattering while $\mathcal{V}_K^\perp$ accounts for the backward scattering.

3. Relaxation and decoherence rates

We describe the dynamics of spin chains coupled to the conduction electrons on the edge states in the SHB within the Bloch–Redfield (BR) approach for open quantum systems weakly coupled to reservoirs [46]. This theory have been applied successfully to describe the inelastic electron spectroscopy [4, 47–49], renormalization of the magnetic anisotropy [50, 51] and the dynamics [6, 7, 13, 21, 23, 25, 49] of magnetic adatoms deposited on a thin decoupling layer. Here we just applied the general expressions of the transition and decoherence rates presented in [25] particularized to the coupling terms (3), (4). For simplicity we assume that the strength of the Kondo interaction J_l is the same for all the atoms in the chain, i.e. $J_l = J$. After a long but straightforward algebra, one can arrive to the following expressions for the transition rates $\Gamma_{MM'}$ from state M to M'

$$\begin{aligned}\Gamma_{MM'} = \frac{\gamma_S(\omega_{M'M})}{4S^2} \sum_{l,l'} [&S^z_{MM'}(l) S^z_{M'M}(l') \\ &+ \mathcal{F}_{l-l'}(k_{\rm F} d)[S^x_{MM'}(l) S^x_{M'M}(l') + S^y_{MM'}(l) S^y_{M'M}(l')]],\end{aligned} \tag{5}$$

where $\mathcal{F}_{l-l'}(\xi) = \cos(2\xi(l - l'))$ and $S^a_{MM'}(l) \equiv \langle M|\hat{S}^a(l)|M'\rangle$ for $a = x, y, z$, and $\hbar\omega_{M'M} = E_{M'} - E_M$. Here we have introduced the energy and temperature-dependent transition rate of a single spin S exchange coupled to

[4] With this notation, $k > 0$ states have $\epsilon_k > \epsilon_{\rm F}$ both for L and R fermions.

Table 1. Quasiparticle scattering channels, leading to spin relaxation in the spin chains, in the edge of QSH insulator depending on the variation of the quasiparticle spin ΔS_z and momentum transfer Δk.

	ΔS_z	Δk
QSH allowed	0	0
QSH allowed	± 1	$2\,k_F$
QSH forbidden	0	$2\,k_F$
QSH forbidden	± 1	0

an electron gas

$$\gamma_S(\omega_{M'M}) = \frac{\pi}{2}(\rho J)^2 S^2 \mathcal{G}(\omega_{M'M}), \tag{6}$$

where $\mathcal{G}(x) = x/(e^{\beta\hbar x} - 1)$, with $\beta = 1/k_B T$ and k_B the Boltzmann constant.

There are two kind of scattering processes leading to decoherence. One of them is the so-called *non-adiabatic decoherence*, which is associated to population scattering and whose rate is given by [46] $\gamma^{\text{nonad.}}_{MM'} = (\sum_{N\neq M}\Gamma_{MN} + \sum_{N\neq M'}\Gamma_{M'N})/2$. Even if population scattering is strictly forbidden ($\gamma^{\text{nonad.}} = 0$), there can be a second source of decoherence, the *adiabatic decoherence*, associated to the loss of phase coherence due to scattering with the itinerant electrons. Following the method outlined in our previous work [25], we obtain the adiabatic decoherence rate

$$\gamma^{\text{ad.}}_{MM'} = \frac{\gamma_S(0)}{8S^2}\left[\left|\sum_l [S^z_{MM}(l) - S^z_{M'M'}(l)]\right|^2 + \sum_{b=x,y}\left|\sum_l (e^{i2k_F dl} S^b_{MM}(l) - e^{-i2k_F dl} S^b_{M'M'}(l))\right|^2\right]. \tag{7}$$

Equations (5) and (7) are the central results of this work. In deriving these two equations we have assumed a constant spin-independent density of states around the Fermi level, $\rho(\epsilon) = \sum_{k\sigma}\delta(\epsilon - \epsilon_{k\sigma}) \approx \rho$. In addition, we have approximated $k(\epsilon) \approx \pm k_F$ [49]. Importantly, both $\Gamma_{MM'}$ and $\gamma^{\text{ad.}}_{MM'}$ contains a spin conserving contribution (involving only $S^z(l)$) associated to forward scattering, and a spin-flip contribution associated only to backward scattering.

We can always classify quasiparticle scattering, responsible of both T_1 and T_2, in terms of the amount of spin exchanged with the spin chain, $\Delta S_z = \pm 1,\ 0$. In one dimension, we can further split quasiparticle scattering in two groups, according to the variation of quasiparticle momentum, $\Delta k \approx 0,\ \pm\ 2k_F$, known as forward and backward scattering respectively. We have thus 4 types of scattering channels, listed in the table 1. Importantly, in the case of quasiparticles at the edge states of the QSH insulators, two of these four channels are forbidden, on account of the spin-momentum locking. This holds regardless of the properties of the spin chain. The rest of the discussion shows that, in addition, the spin-flip backward scattering can also be suppressed in suitably tailored spin chains.

4. Relaxation and decoherence of the spin-uncompensated Néel states

Let us consider an antiferromagnetic spin chain with an odd number of $S = 1/2$ spins, which yields a $S = 1/2$ ground state. The lowest energy states of these chains are staggered Néel-like states, where $S^z_{M,M}(l) \sim (-1)^{l+M}\mathcal{S}(l)$, with $\mathcal{S}(l) \sim 1/2$. Figure 2 shows the relaxation time $T_1(N)$ in units of the lifetime of a single spin coupled to a 1D electron gas, $T_1^{1D} = 1/\gamma_{1/2}(\Delta/\hbar)$, where $\Delta = g\mu_B B$. For clarity reasons, we present only two chains with $N = 3, 7$ spins coupled to either a spin-locked electron gas, labeled with SHB, or to a normal 1D conductor. In all cases, $T_1(N)$ are periodic functions of $k_F d$, with period π. The periodic behavior on $k_F d$ is due to the interference between the plane waves of the conduction electrons scattered at different sites of the spin chain, which acts as a diffraction grating [25]. We find that, for all values of $k_F d$, $T_1(N)$ is larger for the spin-locked case than the normal 1D electron gas. This can be understood right away because, for the $S = 1/2$ doublet, $T_1(N)$ entails a flip-flop spin interaction between the quasiparticle bath and the chain state. In the spin-locked edge states case, this is only allowed in the back-scattering channel, see equation (5).

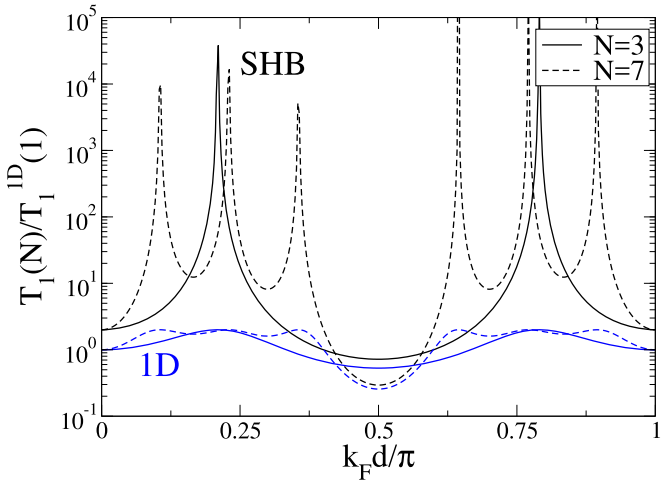

Figure 2. Spin relaxation times for odd $N = 3$ (solid lines) and 7 (dashed lines) $S = 1/2$ spin chains. The relaxation times obtained for the coupling with a SHB (one-dimensional conductor) are depicted in black (blue). In all cases, $J_H = 1$ meV, $g\mu_B B = 0.05$ meV and $k_b T = 0.01$ meV. All times are referred to the relaxation time $T_1^{1D}(1)$ of the single spin.

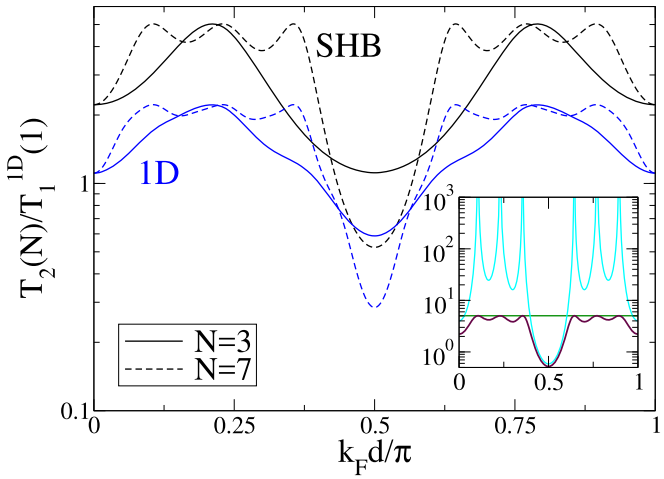

Figure 3. Spin decoherence times $T_2(N)$ for odd $N = 3$ (solid lines) and 7 (dashed lines) $S = 1/2$ spin chains. The decoherence times obtained for the coupling with a SHB (one-dimensional conductor) are depicted in black (blue). Same parameters than in figure 2. The inset shows the adiabatic $1/\gamma^{\text{ad.}}$ (dark green) and non-adibatic $1/\gamma^{\text{nonad.}}$ (cyan) contributions to the total decoherence time $T_2(N)$ (maroon) for the $N = 7$ spin chain.

The most striking feature in figure 2 is the very large modulation of T_1 as a function of $k_F d$, which is dramatically larger for the spin-locked reservoir. By choosing the right values of $k_F d$, one can increase the relaxation time T_1 by more than 4 orders of magnitudes. This control could be achieved either by modifying the inter-spin distance, or by a gate voltage that could vary the Fermi level of the electrode. Notice that, from a practical point of view, changing either d or k_F will probably change the intrachain exchange J, an effect that will not be discussed here. Notice that spin chains of length N presents $N - 1$ maxima of $T_1(N)$ in each period of $k_F d$, with the maxima found when $(k_F d)^{-1} \sim 2(N-1)/\pi$. These maxima in T_1 can be attributed to the suppression of spin-flip back-scattering due to destructive interference in the multiple back-scattering of the quasiparticle with the spin chain. We have verified these findings for chains of length $N = 2n + 1$, with $n \in [1, 10]$.

Let us now consider T_2. The resulting decoherence times $T_2 = 1/(\gamma^{\text{ad.}} + \gamma^{\text{nonad.}})$ are depicted in figure 3. As observed, the SBH case lead to a decoherence time that is roughly a factor 2 larger than the coherence time of the chain coupled to a 1D electron gas. However, for most of the $k_F d$ values, increasing the chain size (and thus, the relaxation times) does not lead to reduction of T_2. The modulation of T_2 with $k_F d$ is very mild, compared to the case of T_1, because the contribution of the spin-conserving forward scattering channel can not be eliminated. This can be seen in the inset of figure 3 where the adiabatic and non-adiabatic contributions to the decoherence time are depicted for the $N = 7$ spin chain. As observed, the (momentum-independent) spin conserving

contribution $1/\gamma^{\mathrm{ad.}}$, see equation (7) and table 1, remains always finite and it dominates the decoherence for most of the $k_F d$ values.

Finally, we should notice that for both coupling to a 1D conductor or to a spin-momentum locked edge state, the relaxation and decoherence times can be substantially larger than for a normal three-dimensional metal with the same density of states at the Fermi energy and the same Kondo coupling [25].

5. Discussion and conclusions

In this work we have explored a new route to boost the spin lifetimes of magnetic atoms on surfaces. To do so, we have taken advantage of the flexibility offered by spin chains by exploring the interference of the quasiparticle scattering at the different positions of the array, combined with the spin-momentum locking of the chiral edge states of a QSH insulator.

In the case of atoms coupled to a normal conductor, spin lifetimes are mainly limited by the Kondo-induced spin-flip processes with quasiparticles at the Fermi surface of the conductor. Therefore, a clear way to increase the spin lifetimes is by reducing the number of scattering channels. This can be achieved for instance in a 1D conductor, where the only allowed processes are forward and backward scattering. Yet, the spin-momentum locking at the borders of a QSH conductor offers an additional thrilling feature: the forward spin-flip channel and the backward spin-conserving channel are fully quenched.

Experimental realizations of magnetic chains placed on the edges of a spin Hall bar are still to be demonstrated. Yet, there are a few substrates candidates such as the monolayer crystals of WTe_2 [34–36] or atomically thin islands of Bi(111) [30, 31]. The advances in STM manipulation and probe together with the STM-induced electron spin resonance makes us think that such an experimental setups could be realized in the near future.

Even if these system can be realized experimentally, there may be some effects preventing the observation of these long relaxation and decoherence times. For instance, we have not explored the possible issues associated with beyond-first neighbors interactions in the chain, and we overlooked the possible RKKY interaction [52]. In addition, we have neglected the role of electron-electron interactions in the SHB, that often has a strong influence in 1D systems.

One natural question that emerges when talking about magnetic atoms on surfaces is the role of magnetic anisotropy and the spin size. Most of the magnetic atoms used for assembly engineered spin structures do not behave as spin $S = 1/2$ systems and they suffer some magnetocrystalline anisotropy [2, 4–8]. We have analyzed the relaxation and decoherence times of anisotropic $S > 1/2$ spin chains, including both longitudinal and transverse anisotropy in the local spin Hamiltonian: $\mathcal{H}(l) = D\hat{S}^z(l)^2 + E[\hat{S}^x(l)^2 - \hat{S}^y(l)^2]$. We verified that for AFM spin chains that can be described as a two level system, a large modulation of T_1 and T_2 times can still be reached by tuning $k_F d$ on a QSH, although results are not as prominent as those of the $S = 1/2$ Heisenberg chain. The corresponding results for a $S = 3/2$ spin chain are shown in appendix B for completeness.

To sum up, spin lifetimes of a $S = 1/2$ spin encoded on odd-numbered antiferromagnetic $S = 1/2$ Heisenberg chains are limited due to Kondo interaction with a substrate. We have shown that this unwanted effect can be dramatically reduced when the Kondo interaction occurs with conduction electrons in the spin-locked edge states of a QSH insulator. This enhancement of the spin lifetimes can be tuned by varying the product $k_F d$ of Fermi wavenumber k_F and inter-spin distance d.We have shown that, for specific values of $k_F d$, the spin-flip backward scattering is also suppressed. This behavior is peculiar of the SHB edge states, and it stands on the locking of the spin and momentum degrees of freedom. Moreover, we demonstrated that although the resulting spin coherence time is limited by the unavoidable spin-conserving forward scattering, it can be still larger than the single spin decoherence time.

Acknowledgments

JFR acknowledges financial support by FCT- The Portuguese Foundation for Science and Technology, under the project 'PTDC/FIS-NAN/4662/2014' (016656), MINECO-Spain (Grant No. MAT2016-78625-C2) and Generalitat Valenciana Prometeo2017/139. FD acknowledges financial support from Spanish Government through grants MAT2015-66888-C3-2-R, Basque Government, grant IT986-16 and Canary Islands program *Viera y Clavijo* (Ref. 2017/0000231). FD acknowledges the hospitality of the Departamento de Física Aplicada of the Universidad de Alicante.

Appendix A. Derivation of the transition rates $\Gamma_{MM'}$

In this appendix we provide some details of the derivation of equation (5). The corresponding equation for the adiabatic decoherence rates can be obtained following the same steps. For convenience we introduced the complex single particle indexes $\alpha \equiv (l, a)$ and $\beta \equiv (l', b)$, where $a, b = x, y, z$. Following the BR approach, we write down the interaction of the quantum system with the bath as $\mathcal{V} = \sum_\alpha R_\alpha \mathcal{S}_\alpha$, where R_α ($\mathcal{S}_\alpha$) are reservoir (system) operators. Using the definitions (3) and (4), we can identify $\mathcal{S}_\alpha \equiv S^a(l)$ and the reservoir operator

$$\begin{aligned} R_\alpha \equiv \frac{J_l}{2L}\sum_{kk'}[&\delta_{a,z}\mathrm{e}^{\mathrm{i}(k-k')dl}(R_k^\dagger R_{k'} - L_{-k}^\dagger L_{-k'}) \\ &+ \delta_{a,x}(\mathrm{e}^{\mathrm{i}(2k_\mathrm{F}+k+k')dl}L_k^\dagger R_{k'} + \mathrm{h.c.}) \\ &+ \delta_{a,y}(\mathrm{ie}^{\mathrm{i}(2k_\mathrm{F}+k+k')dl}L_k^\dagger R_{k'} + \mathrm{h.c.})]. \end{aligned} \tag{A.1}$$

The transition rate $\Gamma_{MM'}$ can be then written in terms of the electrode correlation function $g_\alpha, \beta(\omega)$ in frequency space as [46]

$$\Gamma_{MM'} = \frac{2}{\hbar^2}\sum_{\alpha\beta} g^R_{\alpha,\beta}(\omega_{MM'})\mathcal{S}^{MM'}_\alpha \mathcal{S}^{M'M}_\beta, \tag{A.2}$$

where $g^R_{\alpha,\beta}(\omega_{MM'}) \equiv \mathrm{Re}\,[g_{\alpha,\beta}(\omega_{MM'})]$. For the decoherence rates $\gamma^{\mathrm{ad.}}_{MM'}$ one finds the following expression [46]

$$\gamma^{\mathrm{ad.}}_{MM'} = \frac{2}{\hbar^2}\sum_{\alpha\beta} g^R_{\alpha,\beta}(0)[\mathcal{S}^{M'M'}_\beta - \mathcal{S}^{MM}_\beta][\mathcal{S}^{M'M'}_\alpha - \mathcal{S}^{MM}_\alpha]. \tag{A.3}$$

Hence we only need to evaluate $\mathrm{Re}\,[g_{\alpha,\beta}(\omega)]$ in order to get the relaxation or decoherence rates. The real part of the reservoir correlation function can be written in terms of the matrix elements of R_α[46]:

$$g^R_{\alpha,\beta}(\omega) = \pi\sum_r P_r \sum_{r'}\langle r|R_\alpha|r'\rangle\langle r'|R_\beta|r\rangle\,\delta(\omega - \omega_{rr'}), \tag{A.4}$$

where r, r' label the reservoir states and $P_r = \mathrm{e}^{-\beta\epsilon_r}/Z$ the occupations in the microcanonical ensemble. Working out the expression of the matrix elements in the Slater determinants $|r\rangle$ of the reservoir and introducing the statistical expectation values, one gets for the spin conserving contribution [13, 46]:

$$g^R_{zl,zl'}(\omega) = \frac{\pi J_l J_{l'}}{4L^2}\sum_{kk'} f(\epsilon_k)(1 - f(\epsilon_{k'}))\delta(\omega - \omega_{kk'})\cos[(k - k')d(l - l')]. \tag{A.5}$$

For the spin-flip contribution, we have that $g_{xl,yl'}(\omega) = g_{yl,xl'}(\omega) = 0$, while the diagonal terms are given by

$$g^R_{bl,bl'}(\omega) = \frac{\pi J_l J_{l'}}{4L^2}\sum_{kk'} f(\epsilon_k)(1 - f(\epsilon_{k'}))\delta(\omega - \omega_{kk'})\cos[(2k_\mathrm{F} + k + k')d(l - l')], \tag{A.6}$$

with $b = x, y$. Equations (A.5) and (A.6) are totally general given the Kondo coupling (3), (4). However, in order to get the expression (5) we need to make some extra assumptions. For convenience, we introduce the density of states $\rho(\epsilon) = \sum_{k\sigma}\delta(\epsilon - \epsilon_{k,\sigma})$. In first place, we assume that the density of states is constant and given by its value at the Fermi level, i.e. $\rho(\epsilon) \approx \rho(\epsilon_\mathrm{F}) \equiv \rho$. In second place, as the resulting energy integrand is non-zero only in a small neighborhood of the Fermi level, the momentum-dependent exponentials are approximated by their values at $k = k' = 0$. The resulting energy integration are analytic and one gets the following simple expressions.

$$g^R_{zl,zl'}(\omega) = \frac{\pi J_l J_{l'}}{4L^2}\mathcal{G}(\omega), \tag{A.7}$$

and

$$g^R_{bl,bl'}(\omega) = \frac{\pi J_l J_{l'}}{4L^2}\mathcal{G}(\omega)\cos[2k_\mathrm{F}d(l - l')]. \tag{A.8}$$

Equations (5) and (7) are then trivially found by inserting equations (A.7), (A.8) into expressions (A.2) and (A.3).

Appendix B. Effect of the magnetic anisotropy

Here we illustrate the effects of magnetic anisotropy taking the example of a chain of $S = 3/2$ spins. We choose the parameters of the Hamiltonian so that the there are two low energy states, well separated from the rest, as in the case of the isotropic chain. The results are typify by a chain of size $N = 5$ with $J_H = 0.5|D|$, $E = 0.3|D|$ and $g\mu_\mathrm{B}\mathrm{B}_z = 0.1|D|$. For a small J_H, the ground state would be, to a very good approximation, given by a Néel type product state, where the spins are in the state $|S_z\rangle \propto |+3/2\rangle + \epsilon|-1/2\rangle$ and its time reversal symmetric, with $\epsilon \sim O(\frac{E}{D})$. Antiferromagnetic interaction favors configurations of odd spins pointing in opposite direction

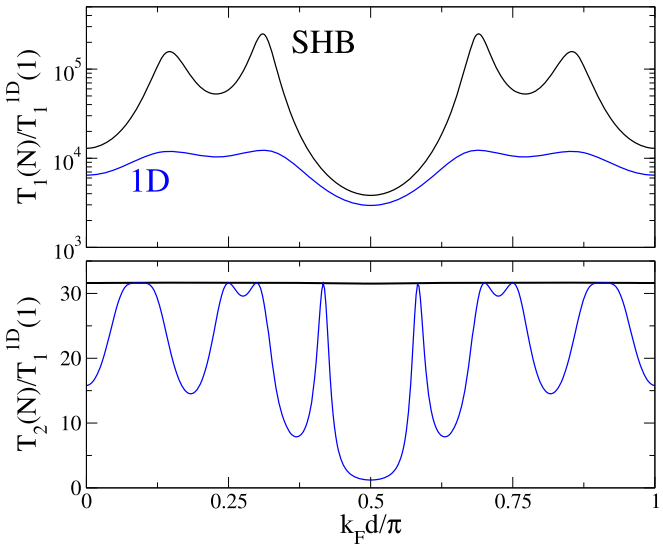

Figure B1. Relaxation times T_1 (top panel) and decoherence times (bottom panel) for an $N = 5$ chain of anisotropic $S = 3/2$ spins versus $k_F d$. The black lines correspond to coupling with a SHB, while blue lines indicates the values for coupling with a one-dimensional conductor. All times are referred to the single spin relaxation time $T_1^{1D} = 1/\gamma_S(1)(\Delta)$. In all cases, $k_B T = 0.01|D|$.

than even spins. The ground state is a doublet that, at finite B_z, is split, defining a two level system. Since J_H is not that small, our low energy doublet has contributions from other configurations as well.

Spin relaxation within this doublet, which determines T_1 and also contributes to the non-adiabatic T_2, occurs via quasiparticle spin-flip, with forward and backward channels. As for the $S = 1/2$ spin chain, the backward channel is modulated by $2k_F d$ and it is the only one available for Kondo coupling with the spin-momentum locked states of the QSH edges, see equations (5) and (7). When $k_F d$ is such that the backward scattering rate drops, T_1 is limited by its residual scattering rate, in contrast to the 1D electron gas that conserve both channels open. The resulting enhancement of T_1 also appears for the anisotropic spin chain, see figure B1.

We now discuss T_2 for the anisotropic spin chain (see bottom panel of figure B1). It has contributions from population scattering, discussed above, and the pure dephasing and spin-preserving contributions. Interestingly, because of the magnetic anisotropy, spin-flip scattering terms are suppressed by a factor ϵ^2, compared to spin-preserving events. Therefore, the latter are dominant. For the QSH case, spin-conserving events are only allowed in the forward scattering channel. As a result, T_2 does not depend on $k_F d$ for the QSH. For the normal case, tuning $k_F d$ can eliminate the backward scattering contributions, making T_2 the same for both types of electron gases.

ORCID iDs

F Delgado https://orcid.org/0000-0003-2180-5273
J Fernández-Rossier https://orcid.org/0000-0003-2297-0289

References

[1] Heinrich A J, Gupta J A, Lutz C P and Eigler D M 2004 *Science* **306** 466–9
[2] Hirjibehedin C F, Lutz C P and Heinrich A J 2006 *Science* **312** 1021
[3] Khajetoorians A A, Chilian B, Wiebe J, Schuwalow S, Lechermann F and Wiesendanger R 2010 *Nature* **467** 1084–7
[4] Loth S, von Bergmann K, Ternes M, Otte A F, Lutz C P and Heinrich A J 2010 *Nat. Phys.* **6** 340–4
[5] Khajetoorians A, Wiebe J, Chilian B and Wiesendanger R 2011 *Science* **332** 1062–4
[6] Loth S, Baumann S, Lutz C P, Eigler D M and Heinrich A J 2012 *Science* **335** 196–9
[7] Spinelli A, Bryant B, Delgado F, Fernández-Rossier J and Otte A 2014 *Nat. Mater.* **13** 782–5
[8] Yang K *et al* 2017 *Phys. Rev. Lett.* **119** 227206
[9] Baumann S, Paul W, Choi T, Lutz C P, Ardavan A and Heinrich A J 2015 *Science* **350** 417–20
[10] Natterer F D, Yang K, Paul W, Willke P, Choi T, Greber T, Heinrich A J and Lutz C P 2017 *Nature* **543** 226–8
[11] Choi T, Paul W, Rolf-Pissarczyk S, Macdonald A J, Natterer F D, Yang K, Willke P, Lutz C P and Heinrich A J 2017 *Nat. Nanotechnol.* **12** 420
[12] Ternes M 2015 *New J. Phys.* **17** 063016
[13] Delgado F and Fernández-Rossier J 2017 *Prog. Surf. Sci.* **92** 40–82
[14] Ternes M 2017 *Prog. Surf. Sci.* **92** 83–115
[15] Hermenau J, Ternes M, Steinbrecher M, Wiesendanger R and Wiebe J 2018 *Nano Lett.* **18** 1978–83

[16] Heinrich B, Braun L, Pascual J and Franke K 2013 *Nat. Phys.* **9** 765–8
[17] Ruggiero C D, Choi T and Gupta J A 2007 *Appl. Phys. Lett.* **91** 253106
[18] Rau I G *et al* 2014 *Science* **344** 988–92
[19] Khajetoorians A A, Lounis S, Chilian B, Costa A T, Zhou L, Mills D L, Wiebe J and Wiesendanger R 2011 *Phys. Rev. Lett.* **106** 037205
[20] Paul W, Yang K, Baumann S, Romming N, Choi T, Lutz C P and Heinrich A J 2017 *Nat. Phys.* **13** 403–7
[21] Miyamachi T *et al* 2013 *Nature* **503** 242–6
[22] Hübner C, Baxevanis B, Khajetoorians A A and Pfannkuche D 2014 *Phys. Rev.* B **90** 155134
[23] Donati F *et al* 2016 *Science* **352** 318–21
[24] Marciani M, Hübner C and Baxevanis B 2017 *Phys. Rev.* B **95** 125433
[25] Delgado F and Fernández-Rossier J 2017 *Phys. Rev.* B **95** 075413
[26] Kane C L and Mele E J 2005 *Phys. Rev. Lett.* **95** 226801
[27] König M, Wiedmann S, Brüne C, Roth A, Buhmann H, Molenkamp L W, Qi X L and Zhang S C 2007 *Science* **318** 766–70
[28] Bernevig B A, Hughes T L and Zhang S C 2006 *Science* **314** 1757–61
[29] Du L *et al* 2017 *Phys. Rev. Lett.* **119** 056803
[30] Drozdov I K, Alexandradinata A, Jeon S, Nadj-Perge S, Ji H, Cava R, Bernevig B A and Yazdani A 2014 *Nat. Phys.* **10** 664
[31] Schindler F *et al* 2018 *Nat. Phys.* **14** 918–24
[32] Yang F *et al* 2012 *Phys. Rev. Lett.* **109** 016801
[33] Kim S H, Jin K H, Park J, Kim J S, Jhi S H, Kim T H and Yeom H W 2014 *Phys. Rev.* B **89** 155436
[34] Fei Z, Palomaki T, Wu S, Zhao W, Cai X, Sun B, Nguyen P, Finney J, Xu X and Cobden D H 2017 *Nat. Phys.* **13** 677
[35] Tang S *et al* 2017 *Nat. Phys.* **13** 683
[36] Wu S, Fatemi V, Gibson Q D, Watanabe K, Taniguchi T, Cava R J and Jarillo-Herrero P 2018 *Science* **359** 76–9
[37] Maciejko J, Liu C, Oreg Y, Qi X L, Wu C and Zhang S C 2009 *Phys. Rev. Lett.* **102** 256803
[38] Lunde A M and Platero G 2012 *Phys. Rev.* B **86** 035112
[39] Zhang F, Kane C L and Mele E J 2013 *Phys. Rev. Lett.* **110** 046404
[40] Tanaka Y, Furusaki A and Matveev K A 2011 *Phys. Rev. Lett.* **106** 236402
[41] Costa M, Nardelli M B, Fazzio A and Costa A 2018 *Longrange dynamical coupling between magnetic adatoms mediated by a 2d topological insulator* arXiv:1808.00347
[42] Meng Q, Vishveshwara S and Hughes T L 2014 *Phys. Rev.* B **90** 205403
[43] Probst B, Virtanen P and Recher P 2015 *Phys. Rev.* B **92** 045430
[44] Silvestrov P G, Recher P and Brouwer P W 2016 *Phys. Rev.* B **93** 205130
[45] Misra P 2007 *Heavy-fermion Systems* vol 2 (Amsterdan: Elsevier)
[46] Breuer H P and Petruccione F 2002 *The Theory of Open Quantum Systems* (Oxford: Oxford University Press)
[47] Fernández-Rossier J 2009 *Phys. Rev. Lett.* **102** 256802
[48] Delgado F, Palacios J J and Fernández-Rossier J 2010 *Phys. Rev. Lett.* **104** 026601
[49] Delgado F and Fernández-Rossier J 2010 *Phys. Rev.* B **82** 134414
[50] Oberg J C, Calvo M R, Delgado F, Moro-Lagares M, Serrate D, Jacob D, Fernández-Rossier J and Hirjibehedin C F 2014 *Nat. Nanotechnol.* **9** 64–8
[51] Delgado F, Hirjibehedin C and Fernández-Rossier J 2014 *Surf. Sci.* **630** 337–42
[52] Zhou L, Wiebe J, Lounis S, Vedmedenko E, Meier F, Blügel S, Dederichs P H and Wiesendanger R 2010 *Nat. Phys.* **6** 187–91